Available online at www.sciencedirect.com
SCIENCE DIRECT®
Agricultural and Forest Meteorology 128 (2005) 243–250
AGRICULTURAL AND FOREST METEOROLOGY
www.elsevier.com/locate/agrformet

Automatic thresholding for hemispherical canopy-photographs based on edge detection

Michael Nobis[a,*], Urs Hunziker[b]

[a]Swiss Federal Research Institute WSL, Zürcherstrasse 111, CH-8903 Birmensdorf, Switzerland
[b]Department of Environmental Sciences, Swiss Federal Institute of Technology Zurich, Chair of Silviculture, ETH Zentrum, CH-8092 Zurich, Switzerland

Received 5 January 2004; received in revised form 11 October 2004; accepted 14 October 2004

Abstract

The analysis of hemispherical photographs is nowadays an established method for assessing light indirectly and describing canopy structures. In this article, we present an automatic threshold algorithm for separating canopy and sky by edge detection. The algorithm was evaluated under different canopy conditions by comparing its results for canopy openness, fractal dimension and diffuse transmittance with those from multiple manual thresholding and direct measurements of the percent photosynthetic photon flux density (PPFD). We show that the automatic threshold algorithm is appropriate to replace the widely used manual interactive processing. It also improves the accuracy of results, especially in comparison with single manual thresholding. Whereas manual threshold setting has often been criticised as subjective and a major source of error the less time-consuming edge detection approach is objective, reproducible and can be applied to a large number of images.

Keywords: Hemispherical photography; Automatic threshold; Digital image processing; Canopy light gaps; Photon flux density; Forest ecosystem

1. Introduction

Light availability is an important site factor in ecology and the management of forests or agricultural land. It can be assessed indirectly in hemispherical photographs, a technique first used for forests by Evans and Coombe (1959) and Anderson (1964), which is nowadays widely applied (recently Bellow and Nair, 2003; Courbaud et al., 2003; Dignan and Bren, 2003; Halverson et al., 2003). With technological progress, several approaches for automation, especially computerised methods, have been proposed (Bonhomme and Chartier, 1972; Olsson et al., 1982; Chan et al., 1986; Chazdon and Field, 1987; Becker et al., 1989). In addition, several software packages for the image analysis are now available (Frazer et al., 2000), and the change from black and white film to digital camera systems has been evaluated (Englund et al., 2000; Frazer et al., 2001; Hale and Edwards, 2002).

* Corresponding author. Tel.: +41 1 739 21 11; fax: +41 1 739 22 15.
E-mail address: michael.nobis@wsl.ch (M. Nobis).

0168-1923/$ – see front matter © 2004 Elsevier B.V. All rights reserved.
doi:10.1016/j.agrformet.2004.10.002

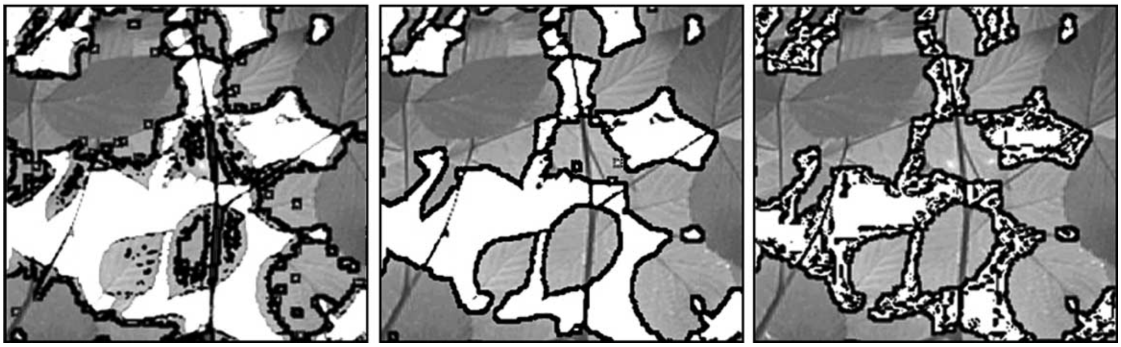

Fig. 1. Positions of edge pixels for different thresholds (for better clarity, the edge pixel pairs are shown in black and enlarged size).

Although using hemispherical photographs has several advantages over direct light assessment and technological and methodological progress have led to improvements in the method, it also has limitations. One of the most critical points is separating the canopy from the sky during image analysis. The usual initial step is a binary transformation generally done by setting a threshold manually, although there are some approaches that work directly with grey or colour values (Olsson et al., 1982; Wagner, 1998, 2001). Several authors have pointed out that manual thresholding can be a relevant source of error because it is somewhat arbitrary and subjective (Chan et al., 1986; Rich, 1990; Machado and Reich, 1999; Frazer et al., 2001; Diaci and Thormann, 2002; Jonckheere et al., 2004).

In this article, we present an automatic threshold algorithm for hemispherical canopy-photographs based on edge detection. The algorithm is evaluated under different canopy conditions by comparing it with single and multiple manual thresholding and direct radiation measurements. The results are discussed in relation to manual thresholding and the known limitations of using hemispherical canopy-photographs to assess radiation indirectly.

2. Methods

2.1. Optimal threshold algorithm

The principle of the method is the search of a threshold value that gives highest local contrast at the edges between classified canopy and sky. Accordingly, the threshold value t with the maximum mean brightness difference at the edges is defined as optimal threshold t_{opt} (Eq. (1); Fig. 1).

$$t_{opt} = \arg\max_{t}\left(\operatorname*{mean}_{S^*}\left\{|b_{x_1,y_1} - b_{x_2,y_2}| \,\middle|\, f(b_{x_1,y_1},t) \neq f(b_{x_2,y_2},t)\right\}\right) \quad (1)$$

$$f(b,t) = \begin{cases} 1 & : \quad b > t \\ 0 & : \quad b \leq t \end{cases} \quad (2)$$

The image domain S^* of calculating the mean is defined as:

$$S^* = \{(x,y) | x \in [1, x_{max} - 1] \wedge y \in [1, y_{max} - 1]\}, \quad (3)$$

with

$$(x_1, y_1, x_2, y_2) \in \{(x, y, x+1, y), (x, y, x, y+1), (x, y, x+1, y+1), (x+1, y, x, y+1)\}. \quad (4)$$

At first, the original photograph (with domain $S = \{(x,y)|x \in [1, x_{max}] \wedge y \in [1, y_{max}]\}$) is transformed into 255 individual images consisting of black and white pixels only, using for each transformation $f(b, t)$ defined by Eq. (2) a different threshold t (here 0–254 according to a single channel of 24-bit-RGB-images), setting brightness values b above t to 1 (white) and those below or equal to 0 (black). On each of the transformed images, a 2×2 moving window defined by Eqs. (3) and (4) is used to average the absolute differences of the corresponding original brightness values b, but only for those pairs of pixels in each window, which in the transformed image represent an edge, i.e. the transformed pixels have different values. The optimal threshold t_{opt} is then defined as that threshold, at which the average brightness difference in the original photograph attains its maximum value. In our equations, the differences within the rightmost pixel column and the bottom pixel row are neglected for simplicity reasons.

The automatic threshold algorithm based on edge detection was implemented using the software SideLook written by M. Nobis (vers. 1.1; www.apple-co.ch). It was first used for the image-based analysis of the vertical vegetation structures in herbaceous stands (Zehm et al., 2003).

2.2. Evaluation

The performance of the automatic threshold algorithm was tested by comparing its results with those obtained using manual thresholding. In the evaluation, a set of 100 images from forests in Switzerland was analysed. The set contains five subsets with 20 images each, covering a broad range of different canopy conditions: (A) uneven-aged mountain forest containing Norway spruce (*Picea abies* (L.) Karst.); (B) even-aged lowland forest containing beech (*Fagus sylvatica* L.); (C) cleared windthrow area; (D) uncleared windthrow area; (E) windthrow-forest edge. The photographs of windthrow areas were taken in lowland beech forests in the third year after the storm damage. In uncleared conditions, the canopies were partly dominated by raspberry (*Rubus idaeus* L.). The images were taken with Nikon Coolpix cameras, using the Nikon Fisheye FC-E8, and recorded in 1:8 or 1:4 JPEG-format (subset A: camera model 995, resolution 2048 pixels × 1536 pixels; subset B–E: model 950, resolution 1600 pixels × 1200 pixels). The blue channel was used for all the image analyses performed. This channel is, in our experience and according to other authors, usually the best one to separate the canopy from the sky (Lee et al., 1983; Frazer et al., 1999, 2001).

Thresholds were first set manually three times in random image order by seven persons, producing 21 manual thresholds per photograph. The software SideLook was used for both the manual and automatic thresholding on seven identical computers and screens. Mean manual thresholds and the thresholds produced by the automatic algorithm were subsequently calculated. The thresholding methods were evaluated by comparing the threshold values, the canopy openness and the fractal dimension of the sky obtained by the two different methods on the same photographs. Canopy openness, defined as uncovered fraction of the sky, and fractal dimension, measured by box counting (Voss, 1988), were calculated with the SideLook software.

In an additional test, the diffuse transmittance calculated after multiple manual and automatic thresholding was compared to the percent photosynthetic photon flux density (% PPFD) measurements in a second set of field data. PPFD (400–700 nm) was measured to quantify diffuse radiation (Parent and Messier, 1996; Comeau et al., 1998; Gendron et al., 1998). During the measurements at dusk, the solar disk was below the horizon and therefore invisible (Diaci and Thormann, 2002). At the time of all measurements, the photon flux density below canopy was not less than 2 $\mu mol\ m^{-2}\ s^{-1}$. The quantum sensors LI-190SA (LI-COR, Lincoln, Nebraska, USA) used give accurate readings at photon flux densities as low as 1 $\mu mol\ m^{-2}\ s^{-1}$ (personal communication; DMP–LI-COR support Switzerland). Two quantum sensors measured the photosynthetic photon flux densities simultaneously. One quantum sensor was used for PPFD-readings below canopy at 22 locations along transect from dense, even-aged Norway spruce forest to a clearing. The second sensor recorded above canopy PPFD-values on a meadow 200 m from the stand. The relation between the two PPFD values, taken at exactly the same time, was calculated to estimate percent PPFD. At the same locations as the below canopy readings, hemispherical images were obtained a few minutes after the PPFD measurements. The photographs were taken in the same way as subset A. Again thresholds were set both manually (five times) and using the automatic algorithm with SideLook. Percent diffuse transmittances were calculated with the software GLA for analysing hemispherical images (Frazer et al., 2000).

3. Results

Fig. 2 shows the comparison of single manual and automatic thresholds with the mean manual threshold values. There are striking scatters for both methods showing similar magnitude of variation. However, the automatic algorithm tends to over- or underestimate the thresholds for the majority of images, this is particularly noticeable for the conifer forest and the uncleared windthrow subsets.

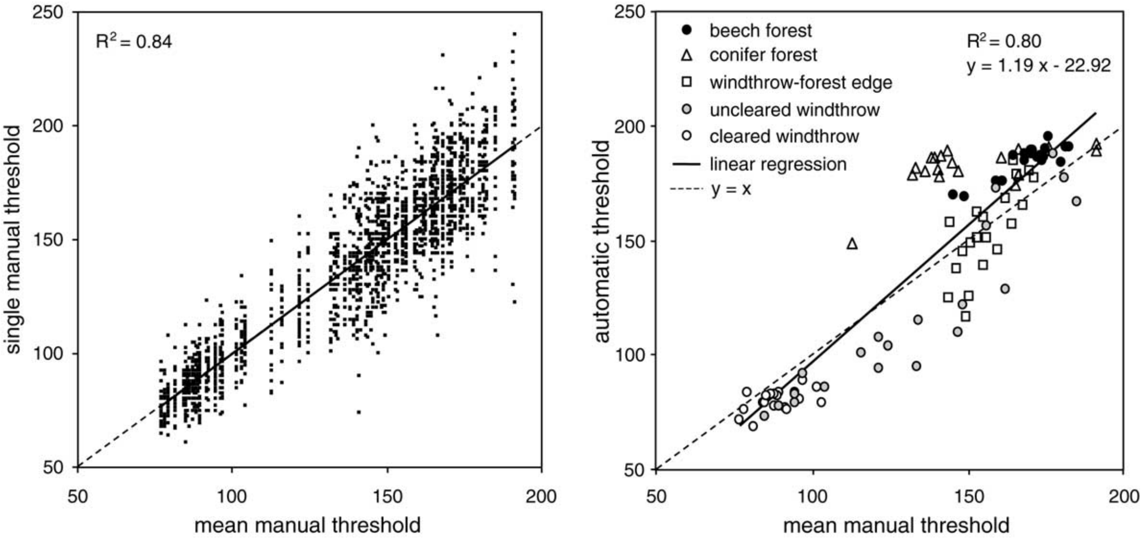

Fig. 2. Scatter plots of the single manual and automatic generated thresholds in relation to the mean manual threshold values.

Results for the canopy openness and fractal dimension are given according to the different thresholding methods in Fig. 3. In contrast to the variation of the raw threshold values, these parameters show very high correlations.

The percent diffuse transmittance of the canopy calculated from digital hemispherical images with the mean manual threshold and the automatic threshold correlated well to measured PPFD values (Fig. 4).

4. Discussion

As shown in Fig. 2, the single manual thresholds vary greatly, which means that they are a potential source of error. Even more parameters calculated after

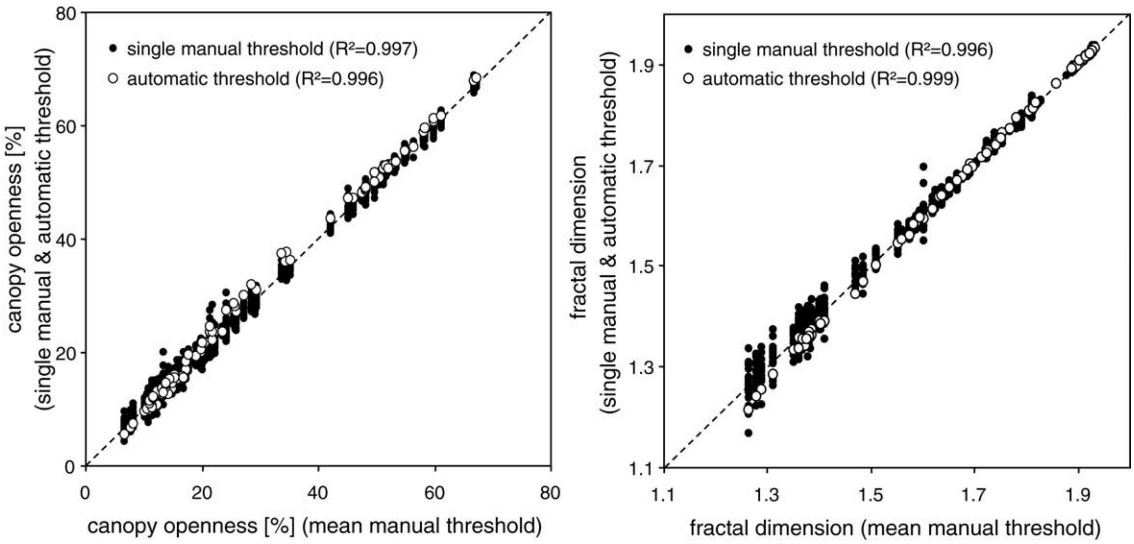

Fig. 3. Comparisons of canopy openness and fractal dimension based on the manual and automatic thresholds.

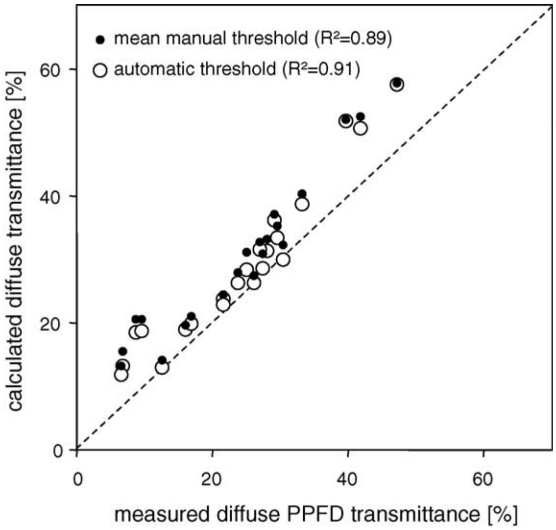

Fig. 4. Comparisons of diffuse transmittance calculated by Gap Light Analyzer software (GLA) for mean manual and automatic thresholds with percent photosynthetic photon flux density (% PPFD). Linear regressions are constrained to pass through the origin.

single manual thresholding may vary remarkably too (Fig. 3). The influence of the variation in single manual thresholds on subsequent analyses depends on both the parameter and the image properties. After transformation, photographs with a high contrast between the vegetation and sky will show only slight differences in a wide range of threshold values, whereas low contrast photographs could result in marked differences. In addition, the influence of the threshold variation caused by manual thresholding may vary not only from parameter to parameter, but also in their range of values. For the low fractal dimensions in Fig. 3, there is a noticeably higher variation in the single manual thresholds than there is for open canopy situations with high fractal dimensions. This increase in variation was not found with the automatic algorithm. Although, there are marked differences between the mean manual thresholds and the automatically generated threshold values (Fig. 2), with both methods, the derived parameters of canopy openness and fractal dimension provided very similar results, whereas single manual thresholding led to a remarkably wider range of values (Fig. 3). Further, the diffuse transmittance calculated after automatic and mean manual threshold setting correlated well with the percent PPFD (Fig. 4). Still the repeatedly reported (Englund et al., 2000; Frazer et al., 2001; Inoue et al., 2002) overestimation of diffuse radiation calculated using digital hemispherical canopy-photographs remains. The results based on automatic thresholds showed slightly lower deviations from the directly measured percent PPFD than the mean manual threshold results (Fig. 4). However, automatic thresholding could not solve the problem of overestimation by digital photographs. The results show that the time-consuming improvement by using the mean manual thresholds instead of single threshold values can be replaced by the automatic processing. Values calculated after automatic thresholding performed at least as good as those calculated using the mean of multiple manual thresholding.

The automatic method has even more advantages, as it is objective and reproducible. We assume that there can be a general and systematic bias in manual thresholding. The manual threshold values tend to be underestimated in canopy photographs characterised by many small canopy gaps, whereas they are, in general, overestimated in windthrow images with wide open canopies and large gaps, but few in number (Fig. 2). This could be explained as a subjective effect depending on whether the processing person focuses either on canopy gaps or on outlines. This assumption is supported by the image subset ‘‘windthrow-forest edge’’ taken within a short time period in the same stand and under constant overcast weather conditions. For this subset, under- and overestimations of the mean manual thresholds in relation to the automatic threshold values clearly correlate with the canopy openness (Fig. 5). This effect can be reproduced and intensified by knowingly focusing either on outlines or small gaps. Moreover, in Fig. 3, the deviation between mean manual and automatic threshold results for low fractal dimensions may be caused by this effect. For open canopies, the deviations in thresholding would be of minor importance for most canopy structure and radiation parameters. For more closed canopies, this together with the variation of single manual thresholds may explain to some extent the finding that hemispherical photography does not work well in dense canopies below 5–10% transmission (Roxburgh and Kelly, 1995; Machado and Reich, 1999; Frazer et al., 2001). It does, however, perform well in more-or-less open sites (Rich et al., 1993; Hale and Edwards, 2002).

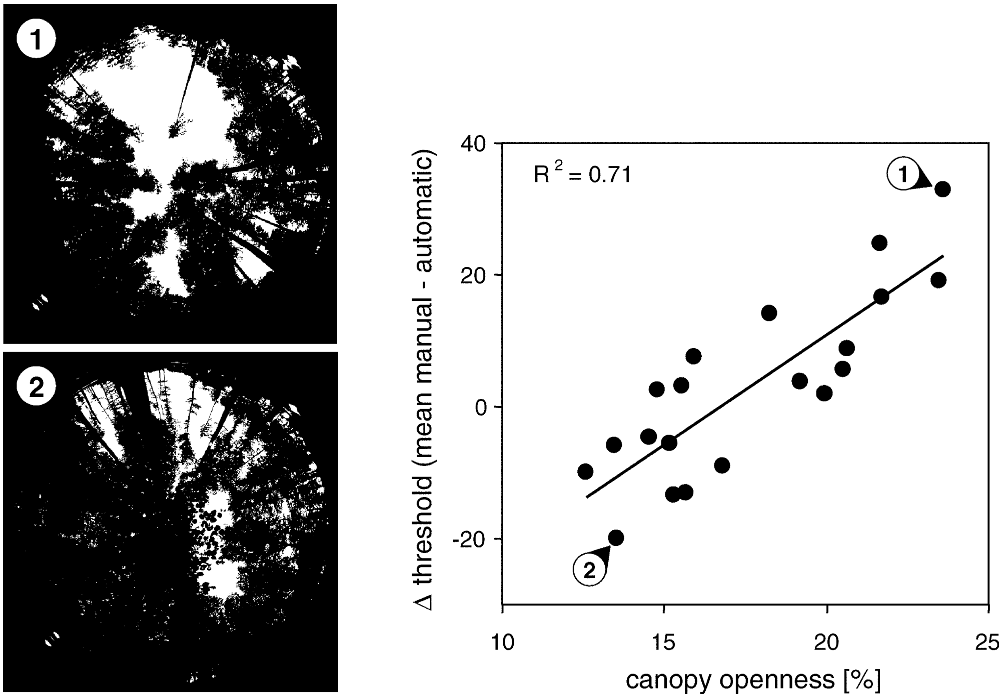

Fig. 5. Differences between mean manual and automatic thresholds against canopy openness. The images correspond to the maximum deviations. Canopy openness was calculated with automatic thresholds.

We assume that for several parameters the automatic threshold method can slightly improve results for dense canopies, but that it cannot solve the limitations of binary canopy/sky images and global thresholding under such situations. Therefore, the automatic thresholding fails not only in dense canopies, but also the binary canopy/sky image approach with global thresholding.

The automatic approach, as described here, has several advantages over manual thresholding. However, in some rarely found situations, the algorithm could initially fail, for example, where there are images with structures of high contrast that do not belong to the border between the vegetation and the sky. This could be caused by the flash or LED (light emitting diodes) signals used in some fisheye applications to identify the north/south orientation of the images. On the other hand, there are photographs with very low contrast showing some apparent artefacts with higher contrasts detected by the algorithm. We assume that this could be caused by JPEG-compression, for example, near to the border of the vegetation and the sky as indicated in Fig. 1 for the overestimated threshold. Both situations are quite rare and the optimal threshold could still be detected by choosing a relative maximum and not the absolute one as described in the methods section.

5. Conclusions

The results show that the suggested automatic threshold algorithm by edge detection has advantages over manual interactive processing. It is objective, comprehensible and reproducible, whereas manual thresholding has often been criticised as subjective and a major source of error. The edge detection approach may also improve the accuracy of the results. But its main advantage is that it is much less time-consuming than manual thresholding and can be applied to a large number of images. For these reasons we think the automatic thresholding method is generally preferable to manual threshold settings, especially where many images are involved.

6. Program source

The automatic threshold algorithm is implemented in the software tool SideLook. It can be downloaded as shareware at http://www.appleco.ch.

Acknowledgements

We are especially grateful to J. B. Stewart and two anonymous reviewers for their valuable comments on the manuscript. The authors would like to thank S. Martin for providing the conifer forest images. We are grateful to C. Dähler, L. von Fellenberg, A. Ghiringhelli, R. Häner, M. de Montmollin and M. Zubler for their help with manual thresholding. We also thank C.W. Hoffmann for his help with mathematical equations and wording. This work was supported by the Swiss Agency for the Environment, Forest and Landscape SAEFL.

References

Anderson, M.C., 1964. Studies of the woodland light climate. 1. The photographic computation of light conditions. J. Ecol. 52, 27–41.

Becker, P., Erhart, D.W., Smith, A.P., 1989. Analysis of forest light environments. 1. Computerized estimation of solar-radiation from hemispherical canopy photographs. Agric. For. Meteorol. 44, 217–232.

Bellow, J.G., Nair, P.K.R., 2003. Comparing common methods for assessing understory light availability in shaded-perennial agroforestry systems. Agric. For. Meteorol. 114, 197–211.

Bonhomme, R., Chartier, P., 1972. Interpretation and automatic measurement of hemispherical photographs to obtain sunlit foliage area and gap frequency. Isr. J. Agric. Res. 22, 53–61.

Chan, S.S., McCreight, R.W., Walstad, J.D., Spies, T.A., 1986. Evaluating forest vegetative cover with computerized analysis of fisheye photographs. Forest Sci. 32, 1085–1091.

Chazdon, R.L., Field, C.B., 1987. Photographic estimation of photosynthetically active radiation: evaluation of a computerized technique. Oecologia 73, 525–532.

Comeau, P.G., Gendron, F., Letchford, T., 1998. A comparison of several methods for estimating light under a paper birch mixedwood stand. Can. J. Forest Res. 28, 1843–1850.

Courbaud, B., de Coligny, F., Cordonnier, T., 2003. Simulating radiation distribution in a heterogeneous Norway spruce forest on a slope. Agric. Forest Meteorol. 116, 1–18.

Diaci, J., Thormann, J.J., 2002. Ein Vergleich verschiedener Lichtmessmethoden in Buchennaturwäldern Sloweniens aus verjüngungsökologischer Sicht. Schweiz. Z. Forestwes. 153, 39–50.

Dignan, P., Bren, L., 2003. A study of the effect of logging on the understorey light environment in riparian buffer strips in a south-east Australian forest. Forest Ecol. Manage. 172, 161–172.

Englund, S.R., O'Brien, J.J., Clark, D.B., 2000. Evaluation of digital and film hemispherical photography and spherical densiometry for measuring forest light environments. Can. J. Forest Res. 30, 1999–2005.

Evans, G.C., Coombe, D.E., 1959. Hemispherical and woodland canopy photography and the light climate. J. Ecol. 47, 103–113.

Frazer, G.W., Canham, C.D., Lertzman, K.P., 1999. Gap light analyzer (GLA): imaging software to extract canopy structure and gap light transmission indices from true-colour fisheye photographs. Users Manual and Program Documentation, Version 2.0, Simon Fraser University, Burnaby, British Columbia, and the Institute of Ecosystem Studies, Millbrook, New York, p. 36.

Frazer, G.W., Canham, C.D., Lertzman, K.P., 2000. Gap light analyzer (GLA), Version 2.0: image-processing software to analyze true-color, hemispherical canopy photographs. Bull. Ecol. Soc. Am. 81, 191–197.

Frazer, G.W., Fournier, R.A., Trofymowc, J.A., Hall, R.J., 2001. A comparison of digital and film fisheye photography for analysis of forest canopy structure and gap light transmission. Agric. For. Meteorol. 109, 249–263.

Gendron, F., Messier, C., Comeau, P.G., 1998. Comparison of various methods for estimating the mean growing season percent photosynthetic photon flux density in forests. Agric. For. Meteorol. 92, 55–70.

Hale, S.E., Edwards, C., 2002. Comparison of film and digital hemispherical photography across a wide range of canopy densities. Agric. For. Meteorol. 112, 51–56.

Halverson, M.A., Skelly, D.K., Kiesecker, J.M., Freidenburg, L.K., 2003. Forest mediated light regime linked to amphibian distribution and performance. Oecologia 134, 360–364.

Inoue, A., Yamamoto, K., Mizoue, N., Kawahara, Y., 2002. Estimation of relative illuminance using digital hemispherical photography. J. For. Plann. 8, 67–70.

Jonckheere, I., Fleck, S., Nackaerts, K., Muys, B., Coppin, P., Weiss, M., Baret, F., 2004. Review of methods for in situ leaf area index determination. Part I. Theories, sensors and hemispherical photography. Agric. For. Meteorol. 121, 19–35.

Lee, Y.J., Alfaro, R.I., Van Sickle, G.A., 1983. Tree-crown defoliation measurement from digitized photographs. Can. J. Forest Res. 13, 956–961.

Machado, J.L., Reich, P.B., 1999. Evaluation of several measures of canopy openness as predictors of photosynthetic photon flux density in deeply shaded conifer-dominated forest understory. Can. J. Forest Res. 29, 1438–1444.

Olsson, L., Carlsson, K., Grip, H., Perttu, K., 1982. Evaluation of forest-canopy photographs with diode-array scanner OSIRIS. Can. J. Forest Res. 12, 822–828.

Parent, S., Messier, C., 1996. A simple and efficient method to estimate microsite light availability under a forest canopy. Can. J. Forest Res. 26, 151–154.

Rich, P.M., Clark, D.B., Clark, D.A., Oberbauer, S.F., 1993. Long-term study of solar-radiation regimes in a tropical wet forest using quantum sensors and hemispherical photography. Agric. For. Meteorol. 65, 107–127.

Rich, P.M., 1990. Characterising plant canopies with hemispherical photographs. Remote Sens. Rev. 5, 13–29.

Roxburgh, J.R., Kelly, D., 1995. Uses and limitations of hemispherical photography for estimating forest light environments. N. Z. J. Ecol. 19, 213–217.

Voss, R.F., 1988. Fractals in nature: from characterization to simulation. In: Peitgen, H.-O., Saupe, D. (Eds.), The Science of Fractal Images. Springer, New York, pp. 21–70.

Wagner, S., 1998. Calibration of grey values of hemispherical photographs for image analysis. Agric. For. Meteorol. 90, 103–117.

Wagner, S., 2001. Relative radiance measurements and zenith angle dependent segmentation in hemispherical photography. Agric. For. Meteorol. 107, 103–115.

Zehm, A., Nobis, M., Schwabe, A., 2003. Multiparameter analysis of vertical vegetation structure based on digital image processing. Flora 198, 142–160.